Intrinsic role of FoxO3a in the development of CD8+ T cell memory

Fanny Tzelepis[1,2], **Julie Joseph**[1,2], **Elias K. Haddad**[5], **Susanne MacLean**[1], **Renu Dudani**[1], **Fabien Agenes**[3], **Stanford L. Peng**[4], **Rafick-Pierre Sekaly**[5], and **Subash Sad**[1,2]

[1]NRC-Institute for Biological Sciences, Canada

[2]University of Ottawa, Department of Biochemistry, Microbiology and Immunology, Canada

[3]INSERM U743, Dept. of Microbiology and Immunology, University of Montreal

[4]Virginia Mason Medical Center, Seattle

[5]Vaccine and Gene Therapy Institute, Florida

Abstract

CD8+ T cells undergo rapid expansion during infection with intracellular pathogens, which is followed by swift and massive culling of primed CD8+ T cells. The mechanisms that govern the massive contraction and maintenance of primed CD8+ T cells are not clear. We show here that the transcription factor, FoxO3a does not influence antigen-presentation and the consequent expansion of CD8+ T cell response during *Listeria monocytogenes* (LM) infection, but plays a key role in the maintenance of memory CD8+ T cells. The effector function of primed CD8+ T cells as revealed by cytokine secretion and CD107a degranulation was not influenced by inactivation of FoxO3a. Interestingly, FoxO3a-deficient CD8+ T cells displayed reduced expression of pro-apoptotic molecules BIM and PUMA during the various phases of response, and underwent reduced apoptosis in comparison to WT cells. A higher number of memory precursor effector cells (MPECs) and memory subsets were detectable in FoxO3a-deficient mice compared to WT mice. Furthermore, FoxO3a-deficient memory CD8+ T cells upon transfer into normal or RAG1-deficient mice displayed enhanced survival. These results suggest that FoxO3a acts in a cell intrinsic manner to regulate the survival of primed CD8+ T cells.

Introduction

CD8+ T cells play a key protective role during infections that are caused by intracellular pathogens (1). After antigenic recognition, naïve antigen-specific CD8+ T cells undergo rapid differentiation into effectors that eliminate infected cells in systemic and peripheral sites (2). Following the peak expansion of CD8+ T cell response, typically day 7, the majority (~95%) of effector CD8+ T cells are swiftly eliminated and only a small proportion of those CD8+ T cells survive (~5%), establishing a long-lived population of memory CD8+ T cells that confer long-term protection against a subsequent encounter with the same pathogen (3–6).

Apoptosis is a key mechanism that promotes the contraction of CD8+ T cell response (7). The extrinsic (death receptor) pathway involves interaction of members of the tumor necrosis factor receptor family (TNFR) with ligands such as FasL, TNF and TRAIL, leading to activation of the caspase cascade which results in cell-death (8,9). In the intrinsic (mitochondrial) pathway, disruption of mitochondrial membrane occurs by the expression or

Correspondence: subash.sad@nrc.ca.

activation of BH3-only family proteins such as BIM, BID and PUMA. This causes the release of cytochrome c that results in activation of caspase 3 and 7 and consequently cell death (10,11). Levels of BIM, PUMA, FasL and TRAIL have been shown to be regulated by the Foxo3a transcription factor, which suggests that Foxo3a can act in both pathways (12–15).

Activation of Foxo promotes nuclear localization, which allows transcription of target genes such as BIM. In contrast, phosphorylation of Foxo proteins by PI3K-Akt (phosphaphatidylinositol 3-kinase-Akt) pathway leads to cytoplasmic localization by association with 14-3-3 protein and eventual degradation (16–18). We have previously shown that the phosphorylation of Foxo3a induced by TCR and c cytokines (IL-2 and IL-7) signalling promotes survival of human CD4^{+} central memory T cells (19). Furthermore, activated Foxo3a was the key mediator of CD4^{+} T cells death in HIV infection (20,21). In murine Lymphocytic choriomeningitis virus (LCMV) infection model, it was showed that Foxo3a deficiency leads to increased expansion, but not contraction, of CD4^{+} and CD8^{+} T cell responses by modulation of the function of dendritic cells (22).

The mechanisms underlying the contraction and maintenance of CD8^{+} T cells are not completely clear. In this study, we have evaluated the role of Foxo3a in the expansion, contraction and maintenance of CD8^{+} T cells during infection with LM. We found that absence of Foxo3a signalling did not significantly influence antigen-presentation or expansion of CD8^{+} T cell response. Inactivation of FoxO3a promoted increased survival of primed CD8^{+} T cells during the contraction phase, resulting in a greater pool of memory CD8^{+} T cells. Furthermore, our data indicates that FoxO3a signalling in CD8^{+} T cells is directly responsible for increased contraction of primed CD8^{+} T cells due to increased expression of pro-apoptotic molecules BIM and PUMA. This is the first time that the intrinsic role of FoxO3a on CD8^{+} T cells during the contraction and maintenance phase has been demonstrated, which highlights the importance of intrinsic pathway in facilitating the elimination of primed CD8^{+} T cells during the contraction phase.

Material and Methods

Mice and infections

All animals were housed in the animal facility of the Institute for Biological Sciences and maintained according to CCAC guidelines. Protocols and procedures (Protocol #2008-10) were approved and monitored by the National Research Council of Canada-Institute for Biological Sciences Animal Care and Ethics Board. Female C57BL/6J and IL-6-deficient (B6.129S6-IL6tm1kopf/J) mice at 6–8 weeks of age were obtained from the Jackson Labs (Bar Harbor, Maine). CD45.1[+] OT-1 and CD45.2[+] OT-1 mice were bred in-house. We derived FoxO3a-deficient mice by disabling Foxo3a allele using the BayGenomics XA026 embryonic stem cell line, which was derived using a gene-trap targeting strategy (23). These mice were backcrossed to B6 background for more than 10 generations. FoxO3a-deficient OT-1 mice were generated by mating OT-1 (CD45.2) mice with FoxO3a-deficient mice. Mice were maintained in the animal facility at the Institute for Biological Sciences (National Research Council of Canada, Ottawa, Canada) in accordance with the guidelines of the Canadian Council on Animal care. For immunizations with LM-OVA, frozen stocks were thawed and diluted in 0.9% NaCl, and mice were inoculated with 1×10^4 LM-OVA suspended in 200 μL of 0.9% NaCl, via the lateral tail vein (i.v.).

Bacterial strains

OVA-expressing *Listeria monocytogenes* (LM-OVA), as described previously (24), was grown in Brain Heart Infusion (BHI) media (DIFCO Laboratories, Detroit MI) to

O.D.$_{600nm}$=0.4–0.8. At mid-log phase, bacteria were harvested and frozen in 20% glycerol and stored at −80°C. Colony forming units were determined by performing serial dilutions on plates.

Bacterial burden

Spleens from infected mice were homogenized in RPMI 1640 medium. Colony forming units were determined by plating 100 μL aliquots of serial ten-fold dilutions in 0.9% saline on BHI-Agar plates.

In vivo cytolytic activity

In vivo cytolytic activity of antigen-specific CD8$^+$ T cells was enumerated as previously described (25,26). Donor spleen-cell suspensions were prepared and red blood cells lysed by ammonium chloride treatment. Cells were split into two aliquots and labelled with CFSE. One aliquot was stained with low concentration of CFSE (0.2μM) and incubated in R8% medium (RPMI + 8% fetal bovine serum). The second aliquot was stained with 10X CFSE (2μM) and incubated with OVA$_{257-264}$ peptide (10 μg/ml) in R8% medium. After 30 min. of incubation, the two aliquots were mixed 1:1 and injected (20×10^6/mouse) into recipient mice that were infected previously with LM-OVA. Non infected recipient mice served as controls. At 24 h after the donor cell transfer, spleens were removed from recipients and the relative numbers of peptide-pulsed versus control donor cells was enumerated according to a previously published equation (26).

ELISPOT assay

Enumeration of IFN- secreting cells was done by ELISPOT assay (27). Briefly, spleen cells were incubated in anti-IFN- antibody coated ELISPOT plates in various numbers (at a final cell density of 5×10^5/well using feeder cells) in the presence of IL-2 (0.1 ng/ml) and media or OVA$_{257-264}$ (5 μg/ml). Incubation lasted 48h. The plates were subsequently washed, incubated with the biotinylated secondary antibody (37°C, 2h) followed by avidin-peroxidase conjugate (room temp., 1 h). Spots were revealed using AEC staining kit (Sigma).

In vivo antigen-presentation

For evaluation of antigen-presentation *in vivo*, CFSE labeled OT-1 cells were injected (5×10^6) into WT or FoxO3a-deficient mice iv. Mice were infected with LM-OVA either before or after OT-1 injection. Four days after the OT-1 cell transfer, spleens were removed from the recipient mice. The presence of donor OT-1 CD8$^+$ T cells (CD45.1$^+$) and the reduction in CFSE intensity of donor cells was evaluated.

Flow cytometry

For evaluation of the fate and phenotype of OVA$_{257-264}$-specific CD8$^+$ T cells *in vivo*, aliquots of cells (5 × 10^6) were incubated in 80μl of PBS plus 1% BSA (PBS-BSA) with anti-CD16/32 at 4°C. After 10 min., cells were stained with H-2K^{b}OVA $_{257-264}$ tetramer-PE (Beckman Coulter, US) and various antibodies (anti-CD8 PercP-Cy5, anti-CD62L APC-Cy7, anti-CD127 PE-Cy7 and anti-KLRG-1 biotin followed by Streptavidin APC) for 30 min. In order to evaluate Ki67 expression, cells were fixed and permeabilized with cytofix/cytoperm buffer (BD) after extracellular staining with anti-CD8 and OVA-tetramer, and stained with Ki67 FITC (BD) for 30 min. All antibodies were obtained from BD Biosciences (Ontario, Canada). Cells were washed with PBS and fixed in 0.5% formaldehyde and acquired on BD FACS Canto flow cytometer. In some experiments CD45.1$^+$ OT-1 cells were adoptively transferred into CD45.2$^+$ recipients, and the transferred cells were tracked after staining cells with anti-CD45.1 antibodies.

Apoptosis assay

For analysis of apoptosis, spleen cells were cultured overnight in RPMI+8% FBS. Aliquots were stained with anti-CD8 antibody and OVA-tetramer as described above. For Annexin V staining, cells were then incubated for 15 min. at room temperature with Annexin V APC (BD) in binding buffer (BD). For Tunnel staining, the *in situ* cell death detection kit, fluorescein (Roche) was used and the procedure was done according to manufacturer's instruction for cell suspension.

Intracellular staining

Aliquots of spleen cells (10×10^6/ml) were stained with anti-CD8 and anti-CD45.2 antibodies for 30 min. on ice as described above. Cells were then washed, reconstituted in R8, plated into 96-well plates (2×10^6/well) and stimulated with $Ova_{257-264}$ peptide (1 μg/ml) in the presence of Golgi-stop (BD Biosciences). After 4 h, cells were harvested, washed, permeabilized and stained for intracellular IL-2 or IFN- using the cytokine staining kit (obtained from BD Biosciences). Staining for CD107a was done after stimulating spleen cells with OVA-peptide for 4 h in the presence of Golgistop and anti-CD107a antibody. Cells were then stained with anti-CD45.1, anti-CD45.2, anti-CD127, anti-KLRG-1 antibodies.

In vitro stimulation of OT-1 cells

OT-1 spleen cells (45.1^+ or 45.2^+) were incubated (100×10^6 cells/flask) with LM-OVA (1×10^2). After 16 – 18 hours, cells were washed, and cultured in media (RPMI + 8% FBS) containing gentamicin (50 μg/mL). Cells were kept in media containing IL-7 (1 ng/ml) for additional time periods with cultures split on a daily basis to avoid overcrowding. $CD8^+$ T cells were purified using magnetic selection beads (Miltenyi Biotech) and injected iv in 200 μL of HBSS through the tail vein.

CD8$^+$ T cell purification and cell sorting

$CD8^+$ T cells were purified from the spleens of WT and FoxO3a-deficient mice using the anti-CD45.2 beads (Stemcell technology, Vancouver). Purified $CD8^+$ T cells (stained with anti-CD8 PE) were then stained with OVA-tetramer-APC. Cells were sorted on MoFlo cell sorter.

Western blotting

Western blotting was performed on whole cell proteins extracted using RIPA buffer. Samples were normalized for cell number and were loaded on SDS-12% polyacrylamide gels. Proteins were then transferred on to a PVDF membrane, blocked with 5% milk and probed with the primary antibody of interest followed by treatment with an appropriate secondary antibody conjugated to horseradish peroxidase. Antibodies against Foxo3a (#2497S), BIM (#2933S), BID (#20003S) and PUMA (#7467S) were purchased from Cell signalling technology. The blots were further developed using an enhanced chemiluminescence substrate (Bio-rad) and bands were identified by exposing the membrane on to an X-ray film (Kodak).

Statistical analysis—The values of samples were compared by One-Way Anova followed by Tukey HSD tests available at the site http://faculty.vassar.edu/lowry/VassarStats.html, or unpaired t-test using Graphpad prism software. The differences were considered significant when the *P* value was <0.05.

Results

Increased maintenance of CD8$^+$ T cell response in FoxO3a-deficient mice

We evaluated the role of Foxo3a in the development of CD8$^+$ T cell response during infection with the intracellular bacterium, LM. To test the role of FoxO3a, we derived mice deficient in Foxo3a by generating mice bearing a disabled Foxo3a allele using the BayGenomics XA026 embryonic stem cell line, which was derived using a gene-trap targeting strategy (23). WT and FoxO3a-deficient (FoxO3a-*trap*) mice were infected with LM-OVA and the magnitude of OVA-specific CD8$^+$ T cell response was evaluated by staining of spleen cells with H-2K^b-OVA tetramers. FoxO3a-trap mice had similar numbers of OVA-specific CD8$^+$ T cells at day 7, but higher numbers at days 15 and 30 post-infection in comparison to WT mice (Fig. 1A, B). The proliferation of OVA-specific CD8$^+$ T cells was similar in WT and FoxO3a-*trap* mice at various time intervals (Fig. 1C). Fate of primed CD8$^+$ T cells has been linked to their relative expression of CD127 (IL-7R) versus KLRG-1 during the priming phase (28). Short-lived effector cells (SLEC) are IL-7R ^{low}KLRG1^{hi}, and memory precursor effector cells (MPEC) are IL-7R ^{hi}KLRG1^{low}. MPECs have a higher ability to proliferate and to self-renew than SLECs (29). Considering the differences observed in the contraction of OVA-specific CD8$^+$ T cells from WT versus FoxO3a-deficient mice, we addressed whether this can be correlated to the differential expression of CD127 and KLRG-1. At day 7 post-infection, the numbers of SLECs and MPECs were similar in WT and FoxO3a-deficient mice (Fig 1D, E). At later time points, the numbers of MPECs in FoxO3a-deficient mice were significantly higher than WT controls (Fig 1E).

We measured the expression of IL-7R versus CD62L, which has been used for segregation of primed CD8$^+$ T cells into effector T cells (Teff, IL-7R ^{low}CD62L^{low}), effector-memory T cells (Tem, IL-7R ^{high}CD62L^{low}) and central-memory T cells (Tcm, IL-7R ^{high}CD62L^{high}) (30,31). These CD8$^+$ T cell subsets differ in their ability to proliferate, to self-renew and to mediate effector function. At day 7 post-infection, OVA-specific CD8$^+$ T cells in the two groups of mice expressed similar levels of CD62L and IL-7R (Fig. 1F, G). Subsequently, increased numbers of memory CD8$^+$ T cells were noted in FoxO3a-deficient mice.

OVA-specific CD8$^+$ T cell response was also evaluated by ELISPOT assay. At day 7 post-infection (peak of response), there was no difference in the magnitude of OVA-specific CD8$^+$ T cell response (Fig. 2A–C) suggesting that FoxO3a does not influence the expansion phase of CD8$^+$ T cell response. Interestingly at subsequent time intervals, higher numbers of OVA-specific CD8$^+$ T cells were detected in the spleen (Fig. 2A), liver (Fig. 2B) and peripheral blood (Fig. 2C) of FoxO3a-deficient mice. Increased CD8$^+$ T cell response observed in Foxo3a-deficient mice was consistent with greater elimination of peptide pulsed targets in FoxO3a-deficient mice in comparison to WT controls (Fig. 2D, E). Both the groups of mice displayed similar, specific cytotoxicity *in vivo* at day 7 (data not shown). WT and FoxO3a-deficient mice did not show any difference in bacterial burden (Fig. 2F), suggesting that the innate immune response in WT and FoxO3a-deficient mice is perhaps similar.

Previously, in a mouse model of LCMV infection, it was reported that FoxO3a regulates IL-6 production by dendritic cells which leads to regulation of T cell survival (22). We therefore compared the expansion and contraction of OVA-specific CD8$^+$ T cell response in WT and IL-6-deficient mice. At days 7 and 30 post-infection both groups of mice displayed similar frequency of OVA-specific CD8$^+$ T cells in the spleen, liver and blood (Fig. S1 A–C). Also, the percentage of OVA-specific CD8$^+$ T cells was similar at day 7 post-infection

(Fig. S1 D). Thus, IL-6 does not seem to play a role in the development of CD8^{+} T cell response during LM-OVA infection.

We measured the expression of cytokines and chemokines in the serum of WT and FoxO3a-deficient mice at the peak (day 3) of LM-OVA infection using a mouse cytokine/chemokine array. The levels of cytokines/chemokines expressed were compared to uninfected controls. There were subtle perturbations in various cytokines/chemokines. Some cytokines (IL-6, IFN-, IL-1a, IL-2, MIG) were elevated in FoxO3a-deficient mice whereas others (G-CSF, IL-1ra, TIMP-1, TNF-a) were elevated in WT mice (Fig. S2 A, B), however, these did not impact the bacterial burden (Fig. 2F).

Loss of Foxo3a does not modulate antigen-presentation

While we failed to note any impact of FoxO3a-deficiency on the development of CD8^{+} T cell response at the peak (day 7), we still considered the possibility that there may be some influence on antigen-presentation. Specifically, we considered the possibility that FoxO3a-deficient mice might display prolonged antigen-presentation that might influence the maintenance of CD8^{+} T cell response subsequently. Control of LM-OVA burden was similar in both the groups (Fig. 2F), implying that the difference in the CD8^{+} T cell response between WT and FoxO3a-deficient mice was not related to bacterial burden. WT and FoxO3a-trap dendritic cells infected with LM-OVA *in vitro* displayed similar antigen-presentation upon culture with CFSE-labelled OT-1 cells (Fig. 3A). To evaluate antigen-presentation *in vivo*, we transferred CFSE labelled OT-1 cells to WT and Foxo3a-deficient mice at various time intervals before or after infection with LM-OVA. Change in the numbers, and CFSE-expression, of transferred OT-1 cells (CD45.1[+]) was evaluated four days post-OT-1-transfer to determine the potency and magnitude of antigen presentation. When OT-1 cells were transferred at days −1 or 5 of infection, WT and FoxO3a-deficient mice displayed potent and similar activation of OT-1 cells (Fig. 3B–E). When OT-1 cells were transferred at day 10 of infection, there was minimal activation of OT-1 cells in both the groups of mice. These results confirm that antigen-presentation against LM-OVA occurs during the first week of infection (32), and this is not affected by the inactivation of FoxO3a.

Intrinsic role of Foxo3a in primed CD8^{+} T cells

We determined whether Foxo3a acts in a cell intrinsic manner to promote the maintenance of primed CD8^{+} T cells. WT and FoxO3a-deficient OT-1 cells were adoptively transferred into naïve WT mice that were infected with LM-OVA. The numbers of OVA-specific CD8^{+} T cells were enumerated at various time intervals by tetramer staining. FoxO3a-deficient OT-1 cells survived in higher proportions in comparison to WT cells (Fig. 4A, B). Endogenous OVA-specific CD8^{+} T cell response is undetectable at late time periods in this model, so the response is mainly comprised of adoptively transferred OT-1 cells. In order to more specifically track the role of FoxO3a in CD8^{+} T cell differentiation, we resorted to a different experimental protocol (Fig. 4C, D) wherein WT OT-1 cells (CD45.1^{+}CD45.2^{+}) were mixed 1:1 (Fig. 4D) with FoxO3a-deficient OT-1 cells (CD45.2[+]) and injected into 45.1[+] (B6.SJL) hosts, which were then infected with LM-OVA (Fig. 4C, D). Using this system, we could track the differentiation and fate of WT and FoxO3a-deficient cells in the same host. Here again, the proportion of FoxO3a-deficient CD8^{+} T cells was significantly higher than WT cells in blood as well as spleen (Fig 4E–J). The proportion of MPECs were also higher in FoxO3a-deficient cells.

It has been previously shown that transgenic CD8^{+} T cells compete with endogenous CD8^{+} T cells for antigen-presentation (33), which influences subsequent differentiation of primed cells (34,35). Therefore, to specifically evaluate the cell intrinsic role of FoxO3a in CD8^{+} T cells we resorted to another experimental model wherein spleen cells (100×10^6) of naïve

WT OT-1 (CD45.1^{+}) and FoxO3a-deficient OT-1 (45.2^{+}) were infected *in vitro* with LM-OVA (10^2). After overnight culture, cells were washed and subsequently cultured in media containing gentamicin to eliminate bacteria. At day 2, CD8^{+} T cells were purified, mixed 1:1 (WT: FoxO3a-trap) and adoptively transferred into naïve WT mice (Fig. S3 A). At day 1 post-transfer, similar numbers of WT and FoxO3a-deficient CD8^{+} T cells were detectable in the spleen (Fig. S3 B). At later time periods, WT OT-1 cells displayed poor survival in comparison to FoxO3a-deficient OT-1 cells (Fig. S3 B). We also cultured the *in vitro* stimulated OT-1 cells (as described above) with IL-7 for 12 days and then transferred them into naïve recipients. Here again, FoxO3a-deficient CD8^{+} T cells displayed increased maintenance in comparison to WT cells (Fig. S3 C, D).

Reduced apoptosis in Foxo3a-deficient CD8^{+} T cells

We determined whether OVA-specific CD8^{+} T cells from FoxO3a-deficient mice displayed better survival than WT counterparts. At day 15 post-infection, we noted reduced expression of Annexin V and TUNEL in OVA-specific CD8^{+} T cells from FoxO3a-deficient mice compared to WT mice (Fig 5A–C). These results indicate that the increased maintenance of OVA-specific CD8^{+} T cells in FoxO3a-deficient mice may be related to their increased survival. Foxo3a transcription factor controls transcription of several downstream gene targets involved in apoptosis (12–15). In order to investigate the mechanisms by which Foxo3a controls the survival of OVA-specific CD8^{+} T cells during LM-OVA infection, we evaluated the expression of pro-apoptotic molecules by western blotting. OVA-specific CD8^{+} T cells were purified by magnetic beads followed by cell sorting, and the expression of pro-apoptotic molecules was examined. While the WT and FoxO3a-deficient, OVA-specific CD8^{+} T cells expressed similar levels of Bid, the expression of Bim and Puma was reduced in FoxO3a-deficient cells at day 7 (Fig. 5D, E). Similar results were noted at subsequent time intervals. As expected, the expression of FoxO3a was un-detectable in FoxO3a-trap mice (Fig. 5D, E). In addition, we also evaluated the expression of Fas receptor and Bcl2 on OVA-specific CD8^{+} T cells at day 15 post-infection and did not notice any significant difference in WT and FoxO3a-trap cells (Fig. 5F, G). The expression of Bcl2 appeared to be slightly lower in FoxO3a-deficient CD8^{+} T cells in both KLRG-1^{hi} and KLRG-1^{low} subsets (Fig. 5G–I). Taken together, these results indicate that FoxO3a-deficient cells undergo reduced cell death following activation *in vivo*.

Foxo3a-deficient CD8^{+} T cells display increased survival

We evaluated the homeostatic proliferation of OVA-specific CD8^{+} T cells from infected WT and FoxO3a-deficient mice. At day 30 post-infection, (Fig. 6A–C), spleen cells were labelled with CFSE and cultured *in vitro* in the presence of IL-7 and IL-15. FoxO3a-deficient cells appeared to display slightly better homeostatic proliferation (Fig. 6B, C), however, the fold-increase in the numbers of OVA-tetramer^{+} CD8^{+} T cells was similar for WT and FoxO3a-deficient cells (data not shown). In order to track the relative proliferation and survival of OVA-specific cells *in vivo*, we transferred purified CD8^{+} T cells at day 90 post-infection into Rag1-deficient mice and evaluated the fate of transferred cells five days later (Fig. S4 A). There was no difference in the proliferation of WT and FoxO3a-deficient memory CD8^{+} T cells at day 5 post-transfer (Fig. S4 B, C). We considered the possibility that the difference in relative survival of cells as a consequence of homeostatic proliferation may manifest at later time intervals post-transfer. Thus, a different experimental protocol was set up in which both WT and FoxO3a-deficient OT-1 cells, differing in CD45.1/CD45.2 expression, were mixed 1:1 and injected into B6.SJL hosts that were then infected with LM-OVA (Fig. 6D). At day 24, CD8+ T cells from these recipients were purified and transferred into naïve Rag1-deficient mice (Fig. 6E). As is indicated in the panel E, the numbers of FoxO3a-trap cells were two-fold greater than WT cells. We then measured the fate of these cells at 30 days post-transfer to Rag-1-deficeint mice (Fig. 6F–H). FoxO3a-deficient, OVA-

specific CD8+ T cells displayed greater cell survival in comparison to WT cells (Fig. 6F, G). When the initial input cell numbers were normalized, even then the increased survival of FoxO3a-deficient cells was evident (Fig. 6H).

The function of CD8^{+} T cells is not influenced by FoxO3a-mutation

We evaluated the expression of IFN- by WT versus FoxO3a-trap, OVA-specific CD8^{+} T cells at day 60 post-infection, and did not notice any difference in the expression of IFN- . (Fig. 7A, B). Similarly, the expression of intracellular IL-2 was not different between WT and FoxO3a-deficient cells (Fig. 7C, D). Furthermore, IL-2 secretion by MPECs was similar in case of WT and FoxO3a-deficient cells (Fig. 7E).

Considering the increased specific cytolytic activity that was detected *in vivo* in FoxO3a-deficient mice (Fig. 1D, E), we wished to determine whether the cytolytic activity of FoxO3a-deficient cells is intrinsically better. Using the CD107a degranulation assay (36) which provides a functional analysis of the cytolytic potential of CD8^{+} T cells, we tested the degranulation of CD107a in WT and FoxO3a-deficient, OVA-specific CD8^{+} T cells at various time intervals post-infection. At day 7, FoxO3a-deficient, OVA-specific CD8^{+} T cells displayed reduced CD107a degranulation, whereas at other time intervals there was similar CD107a degranulation in WT and FoxO3a-deficient CD8^{+} T cells (Fig. 8A, B). Both MPECs and SLECs displayed similar degranulation of CD107a (Fig. 8C, D).

Discussion

CD8^{+} T cells undergo varying level of activation and expansion in different infection models, however, the extent of contraction of the primed CD8^{+} T cells appears to be programmed, as the proportion of cells that contract after priming seems to remain constant (~90%). How the primed CD8^{+} T cells undergo contraction and subsequent maintenance after priming is an area of active investigation. In this report we have addressed the role of the transcription factor FoxO3a in the maintenance of CD8^{+} T cell response during infection with an intracellular bacterium. Our results reveal that FoxO3a acts in a cell intrinsic manner to promote the maintenance of CD8^{+} T cells.

Contraction of CD8^{+} T cell response has been shown to be programmed as contraction continues unaltered even during chronic infections (37). Even when the pathogen burden is prematurely eliminated at 24 h post-infection, contraction of the CD8^{+} T cell response proceeds unaltered (24,32). On the other hand, inflammation has been shown to influence the extent of contraction of CD8^{+} T cell response (38). Infection of IL-15-deficient mice with LM-OVA leads to a higher contraction of CD8^{+} T cell response, while in IL-15 transgenic mice the reverse is observed (39). Administration of IL-7 or IL-15 at the peak of OVA-specific CD8^{+} T cells response in VSV-OVA (vesicular stomatitis virus expressing OVA) or LM-OVA infected mice results in a lower contraction of primed CD8^{+} T cells (40). Interestingly, IL-7 and IL-15 treatment seems to rescue different subsets of CD8^{+} T cells. The numbers of KLRG-1^{hi}CD127^{low} (SLECs) cells were increased by IL-15 administration, while the numbers of KLRG-1^{low}CD127^{hi} (MPECs) and KLRG-1^{hi}CD127^{hi} were increased by IL-7 administration (40). Our results indicate higher numbers of KLRG-1^{hi}CD127^{hi} cells and lower numbers of KLRG-1^{hi}CD127^{low} CD8^{+} T cells in FoxO3a-deficient mice, suggesting a possible coupling between IL-7 signalling and phosphorylation of Foxo3a during LM-OVA infection.

While the appearance of SLECs and MPECs during the differentiation of CD8^{+} T cells has been clearly described previously (28), it is noteworthy that there is another CD8^{+} T cell subset (KLRG-1^{hi}CD127^{hi}) that is increased in FoxO3a-deficient mice. It is conceivable that this is a transitory population that has been rescued from SLECs and is progressing towards

the MPEC phenotype. The proportion of SLECs decreases commensurate with the increase in KLRG-1^{hi}CD127^{hi} cells from day 15 to day 30 in FoxO3a-deficient mice. The characteristics of this population such as proliferation, self renewal, cytokine expression and survival need further investigation.

Foxo3a transcription factor has been involved in the control of different biological processes: regulation of lymphoid homeostasis by inhibition of NF-κB (23), and control of cell proliferation and apoptosis by regulating the transcription of anti-proliferative and pro-apoptotic genes such as p27 and BIM, respectively (12,15,41). Phosphorylation of Foxo3a induces survival of cells in response to oxidative stress (42–44), and survival of CD4$^+$ T cells from normal healthy controls or HIV$^+$ patients (19–21). Our results indicate that the increase in the maintenance of OVA-specific CD8$^+$ T cells in Foxo3a-deficient mice during LM-OVA infection is related to their reduced expression of pro-apoptotic molecules BIM and PUMA, which influences their homeostatic proliferation and survival in the long-term. As Foxo3a regulates the expression of the pro-apoptotic molecules BIM and PUMA in our model, these results agree with previous findings that BIM-deficient mice or BIM-deficient CD8$^+$ T cells have a lower contraction (7,45,46). Furthermore, our results also corroborate previous studies wherein the cooperation between BIM and PUMA in mediating cell-death was demonstrated (47,48). In BIM-deficient mice, the acute contraction of CD8$^+$ T cell response was greater (46) in comparison to our studies with FoxO3a-trap mice. Since we noted that FoxO3a-trap mice displayed a significant reduction, but not complete elimination, of BIM in CD8$^+$ T cells, it is possible that the residual levels of BIM promote a significant level of acute contraction in FoxO3a-trap mice. Alternatively, it is possible that FoxO3a only influences the late stage maintenance of CD8$^+$ T cell response. It is also conceivable that a significant part of what may appear as acute contraction may actually be related to the migration of primed cells from lymphoid to non-lymphoid organs (49). A total lack of contraction may then be achieved only when death of primed cells as well as their migration to other sites is blocked. We did not notice any upregulation of Bcl2, commensurate with reduction in BIM levels in FoxO3a-deficient CD8$^+$ T cells. There was a slight reduction in Bcl2 levels in FoxO3a-deficient CD8$^+$ T cells in comparison to WT cells. This is in agreement with a previous report wherein the levels of BIM and Bcl2 were shown to be interdependent (50).

Our data differs from a previous study in LCMV infection model where Foxo3a was shown to indirectly control the expansion of CD8$^+$ T cells by affecting IL-6 production by DCs, without having any influence during the contraction of the response (22). Recently, another study in the LCMV infection model concluded that FoxO3a acts in a CD8$^+$ T cell-intrinsic manner to promote expansion of CD8$^+$ T cell response (51). FoxO3a was also shown to regulate the expansion of CD8$^+$ T cell response during chronic LCMV infection (52). Thus, there appears to be disagreement regarding the mechanism through which FoxO3a promotes T cell expansion during LCMV infection. Our data indicates that IL-6 does not influence the magnitude of expansion or contraction of CD8$^+$ T cell immune response during LM infection (Fig. S1). While Sullivan et al reported a relatively small increase in the expansion of CD8$^+$ T cell response in FoxO3a-deficient mice, this difference was not noted in the lymphoid organs (51,52). In the LM model, while we noted a small increase in the CD8$^+$ T cell response (at day 7) in FoxO3a-deficient mice in some experiments, this difference was too small and was not significant. Based on the current paradigms of CD8$^+$ T cell differentiation, CD8$^+$ T cells are culled during the contraction, but not the expansion phase of the response (37). It is thus unclear how FoxO3a can modulate the CD8$^+$ T cell expansion in the LCMV model. It is unlikely that the cycling of CD8$^+$ T cells itself is modulated by FoxO3a since WT CD8$^+$ T cells undergo maximal cycling during the expansion phase. Based on the reduction (not complete elimination) of BIM and PUMA levels in FoxO3a-deficient cells, it is likely that FoxO3a influences the contraction of response in a subtle

manner which manifests only at much later time intervals due to continued cell division of the surviving FoxO3a-deficient cells.

Another possible difference between our study and that of Dejean et al (22) is that our mutant mice (Foxo3^{Trap}) were derived by using mutant embryonic cell line obtained from BayGenomics (23), whereas the mutant mice generated by Dejean et al (22) (Foxo3a^{Kca}) were generated with embryonic stem cell clones from the OmniBank embryonic stem cell library. The location of the gene trap splice acceptor in our mice is downstream of the first coding exon, resulting in aberrant splicing of the transcript (23). Consistent with previous analysis of thymus from FoxO3a-trap mice, in which a lack of Foxo3a expression and absence of its truncated forms were reported (23), we failed to detect Foxo3a in purified CD8$^+$T cells from spleen by western blot. Although we cannot completely exclude the possibility that low level of wild-type Foxo3a protein could be present as a result of an alternative splicing around the vector in Foxo3-trap mice, its significance seems minimal due to the clear differences observed in CD8$^+$ T cell survival when compared to wild-type mice. Interestingly, Sullivan et al used the same FoxO3a-trap mice as ours and have noted an intrinsic role of FoxO3a in CD8$^+$ T cell differentiation (51). Thus, it is not clear whether the discrepancy in the intrinsic (51) versus extrinsic (22) role of FoxO3a is related to the source of FoxO3a-deficient mice. Our study has revealed another caveat as the same FoxO3a-deficient mice (51) promote increased maintenance of CD8$^+$ T cell response without having any significant effect during the priming stage. The extent of T cell activation and the subsequent influence of cytokine milieu during viral and bacterial infection are expected to be different. Indeed, it has been previously reported that IFN-I plays a key role in CD8$^+$ T cell expansion during LCMV infection while it has a minimal effect during LM infection (53).

Our data provides novel insights into the key players of the apoptotic pathway that are responsible for promoting contraction and maintenance of CD8$^+$ T cell response after the peak response is generated, thereby creating room for lymphoid homeostasis. These studies reveal new avenues for vaccine development, particularly against cancer therapy, where modulation of Foxo3a phosphorylation can lead to a higher survival of primed CD8$^+$ T cells which may improve vaccine efficacy.

Supplementary Material

Refer to Web version on PubMed Central for supplementary material.

Acknowledgments

Reference List

1. Kaech SM, Wherry EJ, Ahmed R. Effector and memory T-cell differentiation: implications for vaccine development. Nat Rev Immunol. 2002; 2:251–262. [PubMed: 12001996]

2. Prlic M, Williams MA, Bevan MJ. Requirements for CD8 T-cell priming, memory generation and maintenance. Curr Opin Immunol. 2007; 19:315–319. [PubMed: 17433873]

3. Ahmed R, Gray D. Immunological memory and protective immunity: understanding their relation. Science. 1996; 272:54–60. [PubMed: 8600537]

4. Sprent J, Tough DF. T cell death and memory. Science. 2001; 293:245–248. [PubMed: 11452113]

5. Wong P, Pamer EG. CD8 T cell responses to infectious pathogens. Annu Rev Immunol. 2003; 21:29–70. [PubMed: 12414723]

6. Williams MA, Bevan MJ. Effector and memory CTL differentiation. Annu Rev Immunol. 2007; 25:171–192. [PubMed: 17129182]

7. Pellegrini M, Belz G, Bouillet P, Strasser A. Shutdown of an acute T cell immune response to viral infection is mediated by the proapoptotic Bcl-2 homology 3-only protein Bim. Proc Natl Acad Sci U S A. 2003; 100:14175–14180. [PubMed: 14623954]

8. Budihardjo I, Oliver H, Lutter M, Luo X, Wang X. Biochemical pathways of caspase activation during apoptosis. Annu Rev Cell Dev Biol. 1999; 15:269–290. [PubMed: 10611963]

9. Strasser A, O'Connor L, Dixit VM. Apoptosis signaling. Annu Rev Biochem. 2000; 69:217–245. [PubMed: 10966458]

10. Strasser A. The role of BH3-only proteins in the immune system. Nat Rev Immunol. 2005; 5:189–200. [PubMed: 15719025]

11. Suen DF, Norris KL, Youle RJ. Mitochondrial dynamics and apoptosis. Genes Dev. 2008; 22:1577–1590. [PubMed: 18559474]

12. Stahl M, Dijkers PF, Kops GJ, Lens SM, Coffer PJ, Burgering BM, Medema RH. The forkhead transcription factor FoxO regulates transcription of p27Kip1 and Bim in response to IL-2. J Immunol. 2002; 168:5024–5031. [PubMed: 11994454]

13. Modur V, Nagarajan R, Evers BM, Milbrandt J. FOXO proteins regulate tumor necrosis factor-related apoptosis inducing ligand expression. Implications for PTEN mutation in prostate cancer. J Biol Chem. 2002; 277:47928–47937. [PubMed: 12351634]

14. Barthelemy C, Henderson CE, Pettmann B. Foxo3a induces motoneuron death through the Fas pathway in cooperation with JNK. BMC Neurosci. 2004; 5:48. [PubMed: 15569384]

15. Sunters A, Fernandez dM, Stahl M, Brosens JJ, Zoumpoulidou G, Saunders CA, Coffer PJ, Medema RH, Coombes RC, Lam EW. FoxO3a transcriptional regulation of Bim controls apoptosis in paclitaxel-treated breast cancer cell lines. J Biol Chem. 2003; 278:49795–49805. [PubMed: 14527951]

16. Biggs WH III, Meisenhelder J, Hunter T, Cavenee WK, Arden KC. Protein kinase B/Akt-mediated phosphorylation promotes nuclear exclusion of the winged helix transcription factor FKHR1. Proc Natl Acad Sci U S A. 1999; 96:7421–7426. [PubMed: 10377430]

17. Brunet A, Bonni A, Zigmond MJ, Lin MZ, Juo P, Hu LS, Anderson MJ, Arden KC, Blenis J, Greenberg ME. Akt promotes cell survival by phosphorylating and inhibiting a Forkhead transcription factor. Cell. 1999; 96:857–868. [PubMed: 10102273]

18. Maiese K, Chong ZZ, Hou J, Shang YC. The "O" class: crafting clinical care with FoxO transcription factors. Adv Exp Med Biol. 2009; 665:242–260. [PubMed: 20429429]

19. Riou C, Yassine-Diab B, Van Grevenynghe J, Somogyi R, Greller LD, Gagnon D, Gimmig S, Wilkinson P, Shi Y, Cameron MJ, Campos-Gonzalez R, Balderas RS, Kelvin D, Sekaly RP, Haddad EK. Convergence of TCR and cytokine signaling leads to FOXO3a phosphorylation and drives the survival of CD4+ central memory T cells. J Exp Med. 2007; 204:79–91. [PubMed: 17190839]

20. Van Grevenynghe J, Procopio FA, He Z, Chomont N, Riou C, Zhang Y, Gimmig S, Boucher G, Wilkinson P, Shi Y, Yassine-Diab B, Said EA, Trautmann L, El Far M, Balderas RS, Boulassel MR, Routy JP, Haddad EK, Sekaly RP. Transcription factor FOXO3a controls the persistence of memory CD4(+) T cells during HIV infection. Nat Med. 2008; 14:266–274. [PubMed: 18311149]

21. Dabrowska A, Kim N, Aldovini A. Tat-induced FOXO3a is a key mediator of apoptosis in HIV-1-infected human CD4+ T lymphocytes. J Immunol. 2008; 181:8460–8477. [PubMed: 19050264]

22. Dejean AS, Beisner DR, Ch'en IL, Kerdiles YM, Babour A, Arden KC, Castrillon DH, DePinho RA, Hedrick SM. Transcription factor Foxo3 controls the magnitude of T cell immune responses by modulating the function of dendritic cells. Nat Immunol. 2009; 10:504–513. [PubMed: 19363483]

23. Lin L, Hron JD, Peng SL. Regulation of NF-kappaB, Th activation, and autoinflammation by the forkhead transcription factor Foxo3a. Immunity. 2004; 21:203–213. [PubMed: 15308101]

24. Dudani R, Chapdelaine Y, Faassen HH, Smith DK, Shen H, Krishnan L, Sad S. Multiple mechanisms compensate to enhance tumor-protective CD8(+) T cell response in the long-term despite poor CD8(+) T cell priming initially: comparison between an acute versus a chronic

intracellular bacterium expressing a model antigen. J Immunol. 2002; 168:5737–5745. [PubMed: 12023374]

25. Tzelepis F, de Alencar BC, Penido ML, Gazzinelli RT, Persechini PM, Rodrigues MM. Distinct kinetics of effector CD8+ cytotoxic T cells after infection with Trypanosoma cruzi in naive or vaccinated mice. Infect Immun. 2006; 74:2477–2481. [PubMed: 16552083]

26. Barber DL, Wherry EJ, Ahmed R. Cutting edge: rapid in vivo killing by memory CD8 T cells. J Immunol. 2003; 171:27–31. [PubMed: 12816979]

27. Vijh S, Pamer EG. Immunodominant and subdominant CTL responses to Listeria monocytogenes infection. J Immunol. 1997; 158:3366–3371. [PubMed: 9120295]

28. Joshi NS, Cui W, Chandele A, Lee HK, Urso DR, Hagman J, Gapin L, Kaech SM. Inflammation directs memory precursor and short-lived effector CD8(+) T cell fates via the graded expression of T-bet transcription factor. Immunity. 2007; 27:281–295. [PubMed: 17723218]

29. Joshi NS, Kaech SM. Effector CD8 T cell development: a balancing act between memory cell potential and terminal differentiation. J Immunol. 2008; 180:1309–1315. [PubMed: 18209024]

30. Sallusto F, Lenig D, Forster R, Lipp M, Lanzavecchia A. Two subsets of memory T lymphocytes with distinct homing potentials and effector functions [see comments]. Nature. 1999; 401:708–712. [PubMed: 10537110]

31. Wherry EJ, Teichgraber V, Becker TC, Masopust D, Kaech SM, Antia R, von Andrian UH, Ahmed R. Lineage relationship and protective immunity of memory CD8 T cell subsets. Nat Immunol. 2003; 4:225–234. [PubMed: 12563257]

32. Mercado R, Vijh S, Allen SE, Kerksiek K, Pilip IM, Pamer EG. Early programming of T cell populations responding to bacterial infection. J Immunol. 2000; 165:6833–6839. [PubMed: 11120806]

33. Kedl RM, Rees WA, Hildeman DA, Schaefer B, Mitchell T, Kappler J, Marrack P. T cells compete for access to antigen-bearing antigen-presenting cells. J Exp Med. 2000; 192:1105–1113. [PubMed: 11034600]

34. van Faassen H, Saldanha M, Gilbertson D, Dudani R, Krishnan L, Sad S. Reducing the stimulation of CD8+ T cells during infection with intracellular bacteria promotes differentiation primarily into a central (CD62L(high)CD44(high)) subset. J Immunol. 2005; 174:5341–5350. [PubMed: 15843531]

35. Badovinac VP, Haring JS, Harty JT. Initial T cell receptor transgenic cell precursor frequency dictates critical aspects of the CD8(+) T cell response to infection. Immunity. 2007; 26:827–841. [PubMed: 17555991]

36. Betts MR, Brenchley JM, Price DA, De Rosa SC, Douek DC, Roederer M, Koup RA. Sensitive and viable identification of antigen-specific CD8+ T cells by a flow cytometric assay for degranulation. J Immunol Methods. 2003; 281:65–78. [PubMed: 14580882]

37. Badovinac VP, Porter BB, Harty JT. Programmed contraction of CD8(+) T cells after infection. Nat Immunol. 2002; 3:619–626. [PubMed: 12055624]

38. Haring JS V, Badovinac P, Harty JT. Inflaming the CD8+ T cell response. Immunity. 2006; 25:19–29. [PubMed: 16860754]

39. Yajima T, Yoshihara K, Nakazato K, Kumabe S, Koyasu S, Sad S, Shen H, Kuwano H, Yoshikai Y. IL-15 regulates CD8+ T cell contraction during primary infection. J Immunol. 2006; 176:507–515. [PubMed: 16365444]

40. Rubinstein MP, Lind NA, Purton JF, Filippou P, Best JA, McGhee PA, Surh CD, Goldrath AW. IL-7 and IL-15 differentially regulate CD8+ T-cell subsets during contraction of the immune response. Blood. 2008; 112:3704–3712. [PubMed: 18689546]

41. Nakao T, Geddis AE, Fox NE, Kaushansky K. PI3K/Akt/FOXO3a pathway contributes to thrombopoietin-induced proliferation of primary megakaryocytes in vitro and in vivo via modulation of p27(Kip1). Cell Cycle. 2008; 7:257–266. [PubMed: 18256550]

42. Kops GJ, Dansen TB, Polderman PE, Saarloos I, Wirtz KW, Coffer PJ, Huang TT, Bos JL, Medema RH, Burgering BM. Forkhead transcription factor FOXO3a protects quiescent cells from oxidative stress. Nature. 2002; 419:316–321. [PubMed: 12239572]

43. Chong ZZ, Li F, Maiese K. Group I metabotropic receptor neuroprotection requires Akt and its substrates that govern FOXO3a, Bim, and beta-catenin during oxidative stress. Curr Neurovasc Res. 2006; 3:107–117. [PubMed: 16719794]

44. Shang YC, Chong ZZ, Hou J, Maiese K. Wnt1, FoxO3a, and NF-kappaB oversee microglial integrity and activation during oxidant stress. Cell Signal. 2010; 22:1317–1329. [PubMed: 20462515]

45. Wojciechowski S, Jordan MB, Zhu Y, White J, Zajac AJ, Hildeman DA. Bim mediates apoptosis of CD127(lo) effector T cells and limits T cell memory. Eur J Immunol. 2006; 36:1694–1706. [PubMed: 16761315]

46. Prlic M, Bevan MJ. Exploring regulatory mechanisms of CD8+ T cell contraction. Proc Natl Acad Sci U S A. 2008; 105:16689–16694. [PubMed: 18946035]

47. You H, Pellegrini M, Tsuchihara K, Yamamoto K, Hacker G, Erlacher M, Villunger A, Mak TW. FOXO3a-dependent regulation of Puma in response to cytokine/growth factor withdrawal. J Exp Med. 2006; 203:1657–1663. [PubMed: 16801400]

48. Erlacher M, Labi V, Manzl C, Bock G, Tzankov A, Hacker G, Michalak E, Strasser A, Villunger A. Puma cooperates with Bim, the rate-limiting BH3-only protein in cell death during lymphocyte development, in apoptosis induction. J Exp Med. 2006; 203:2939–2951. [PubMed: 17178918]

49. Marshall DR, Turner SJ, Belz GT, Wingo S, Andreansky S, Sangster MY, Riberdy JM, Liu T, Tan M, Doherty PC. Measuring the diaspora for virus-specific CD8+ T cells. Proc Natl Acad Sci U S A. 2001; 98:6313–6318. [PubMed: 11344265]

50. Jorgensen TN, McKee A, Wang M, Kushnir E, White J, Refaeli Y, Kappler JW, Marrack P. Bim and Bcl-2 mutually affect the expression of the other in T cells. J Immunol. 2007; 179:3417–3424. [PubMed: 17785775]

51. Sullivan JA, Kim EH, Plisch EH, Peng SL, Suresh M. FOXO3 regulates CD8 T cell memory by T cell-intrinsic mechanisms. PLoS Pathog. 2012; 8:e1002533. [PubMed: 22359505]

52. Sullivan JA, Kim EH, Plisch EH, Suresh M. FOXO3 regulates the CD8 T cell response to a chronic viral infection. J Virol. 2012; 86:9025–9034. [PubMed: 22675000]

53. Thompson LJ, Kolumam GA, Thomas S, Murali-Krishna K. Innate inflammatory signals induced by various pathogens differentially dictate the IFN-I dependence of CD8 T cells for clonal expansion and memory formation. J Immunol. 2006; 177:1746–1754. [PubMed: 16849484]
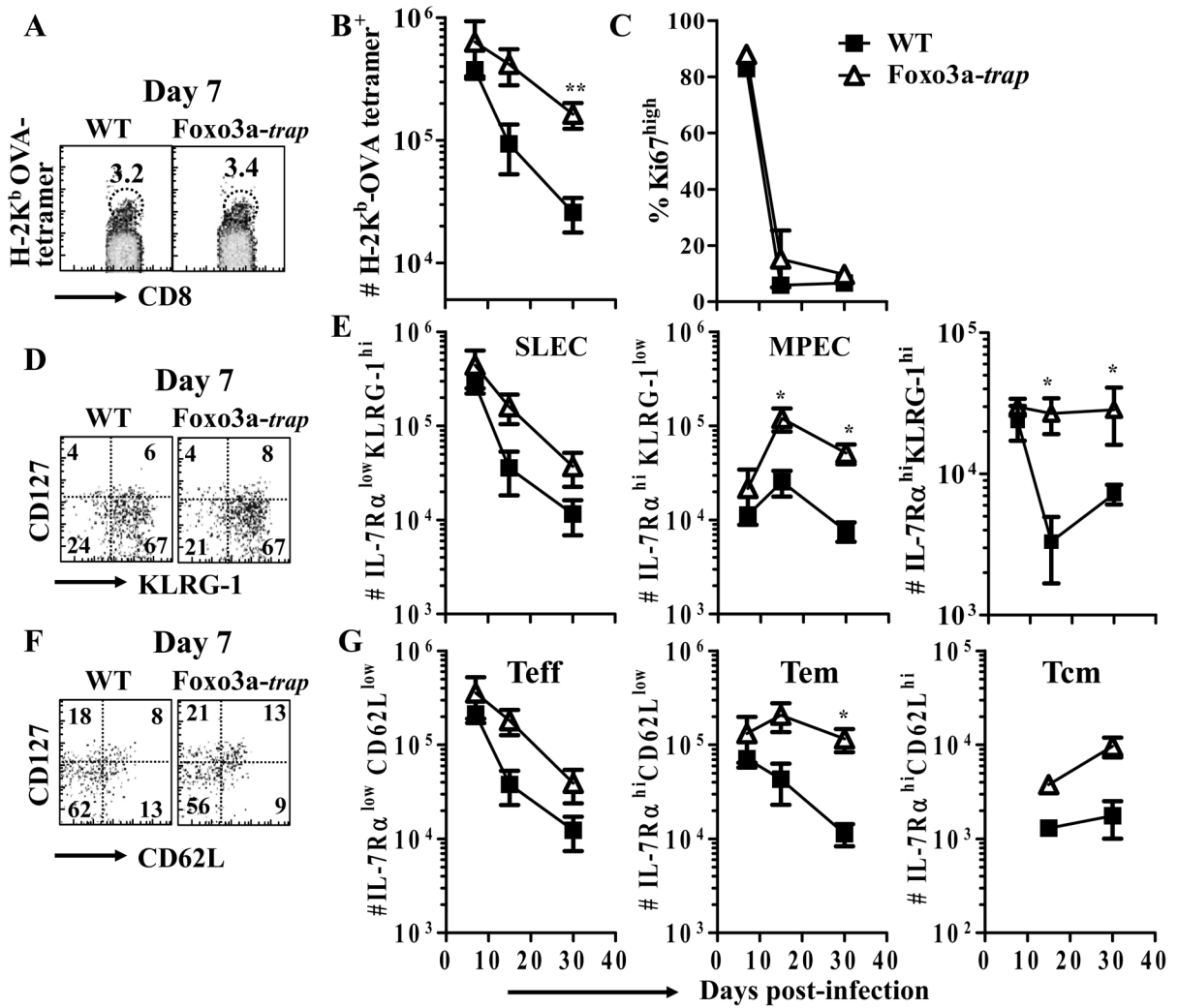
Fig. 1. Increased maintenance of OVA-specific CD8$^+$ T cells in FoxO3a-deficient mice
WT and FoxO3a-deficient mice were infected (iv) with 10^4 LM-OVA. At various time intervals, spleens were isolated from infected mice and spleen cells stained with OVA-tetramer and antibodies against CD8, CD62L, IL-7R , Ki-67 and KLRG-1. Panels A and B show the percentage and total number of OVA-specific CD8$^+$ T cells, respectively. Panel C shows the percentage of Ki67$^+$ OVA-specific CD8$^+$ T cells. The relative expression of IL-7R versus KLRG-1 (D) or CD62L (F) in OVA-specific CD8$^+$ T cells was evaluated. Panel E shows the total numbers of short lived effector cells (SLECs) and memory precursor effector cells (MPECs) based on the expression of IL-7R and KLRG-1 in OVA-specific CD8$^+$ T cells. The total numbers of differentiated OVA-specific CD8$^+$ T cells based on the expression of IL-7R and CD62L is showed in panel G. Teff = effector T cells, Tem = effector memory T cells and Tcm = central memory T cells. Results are representative of two independent experiments with two-three mice per group (* *p<0.05*, ** *p<0.01*).
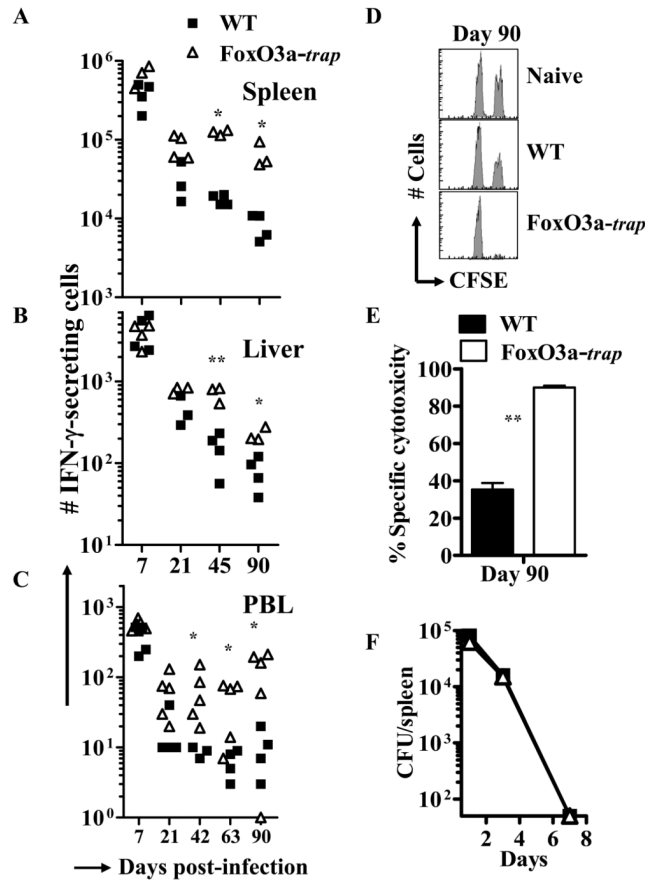
Fig. 2. Increased maintenance of functional CD8^{+} T cells in FoxO3a-deficient mice
WT and FoxO3a-deficient mice were infected (iv) with 10^4 LM-OVA. Frequency of OVA-specific, IFN- -secreting CD8^{+} T cells from entire spleen (A), liver (B, per 10^6 cells) and blood (C, per 5×10^5 cells) was evaluated by ELISPOT assay at various time intervals post-infection. CFSE-labelled, OVA-pulsed and control spleen cells from naïve mice were transferred to naïve or infected mice at day 90, and the specific killing of OVA-pulsed targets was evaluated 24 h later (D, E). Mice were infected with LM-OVA (10^4, iv) and bacterial burden was evaluated at various time intervals by plating serial dilutions of splenic homogenates on BHI-agar plates (F). Results represent the mean of three to five mice ± SD per group and are representative of two independent experiments (** *p<0.01* and * *p<0.05).*
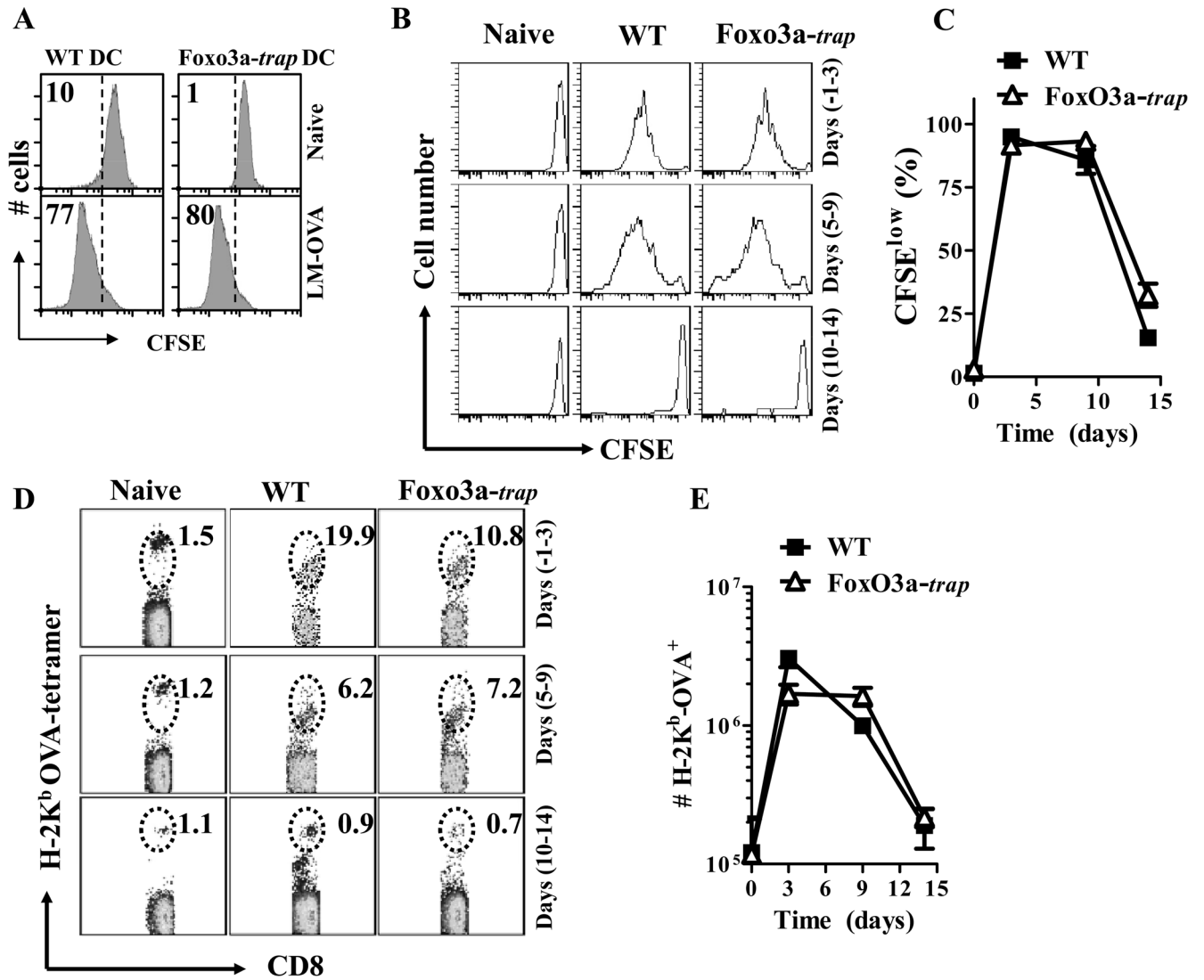
Fig. 3. Similar *in vivo* antigen-presentation in WT and FoxO3a-deficient mice

BMDC (5×10^4) from WT and FoxO3a-deficient mice were infected with 20 MOI of LM-OVA for 30 min. or left uninfected. Extracellular bacteria were removed after washing and incubation in medium containing gentamicin (50 μg/ml). At the end of 2 h, cells were cultured in media containing lower levels of gentamicin (10 μg/ml) and incubated with CFSE labelled OT-1 TCR transgenic cells (10^6/well). After 3 days of culture, cells were harvested, stained with anti-CD8 antibody, and the reduction in CFSE intensity of OT-1 CD8$^+$ T cells was evaluated by flow cytometry (A). WT and FoxO3a-deficient mice were infected (iv) with 10^4 LM-OVA. At various time intervals CFSE-labelled OT-1 CD8$^+$ T cells were injected (5×10^6, iv). Four days after the transfer of OT-1 cells, spleens were isolated from recipient mice and spleen cells were stained with OVA-tetramer and anti-CD8 antibody. Reduction of CFSE expression (B, C) and increase in the numbers of transferred OT-1 cells (D, E) was evaluated. Numbers in the panels represent percentage of OVA-tetramer$^+$ cells within the gate. Results are representative of two independent experiments with three mice per group.
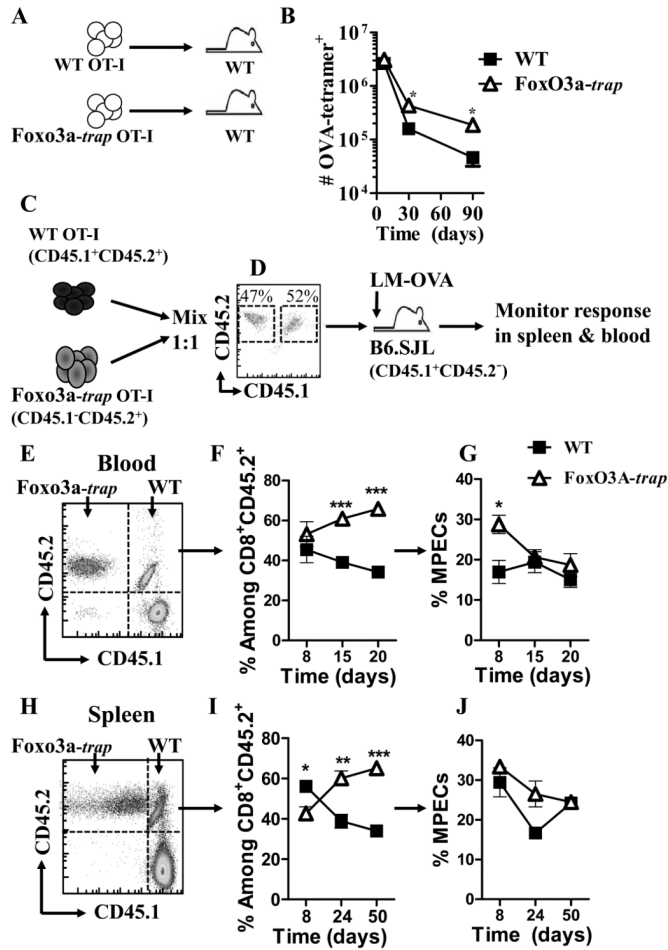
Fig. 4. Intrinsic role of FoxO3a in CD8$^+$ T cells
WT and FoxO3a-deficient OT-1 cells were injected (10^4, iv) into naïve WT mice which were then challenged with 10^4 LM-OVA (iv) immediately thereafter (A). At various time intervals, spleens were removed from infected mice and the relative numbers of OVA-tetramer$^+$ CD8$^+$ T cells evaluated from 3 mice per group (B). WT OT-1 (CD45.1$^+$CD45.2$^+$) cells were mixed 1:1 with FoxO3a-deficient OT-1 (CD45.1$^-$CD45.2$^+$) cells, and injected (iv, 10^4/mouse) into WT (CD45.1$^+$CD45.2$^-$) mice (C), followed by infection with LM-OVA as described above. The numbers and phenotype of OVA-specific CD8$^+$ T cells was tracked in the blood (E–G) and spleen (H–J) of infected mice with antibodies against CD8, CD45.1, CD45.2, CD127 and KLRG1.
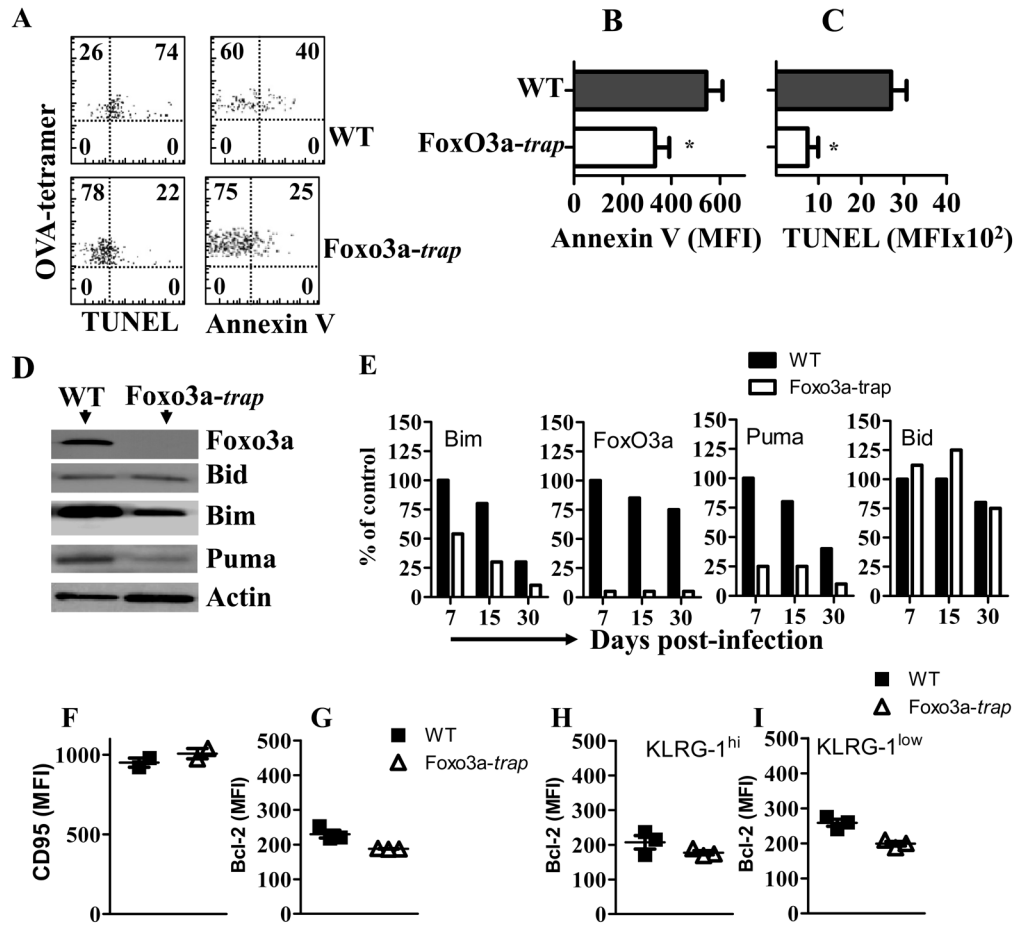
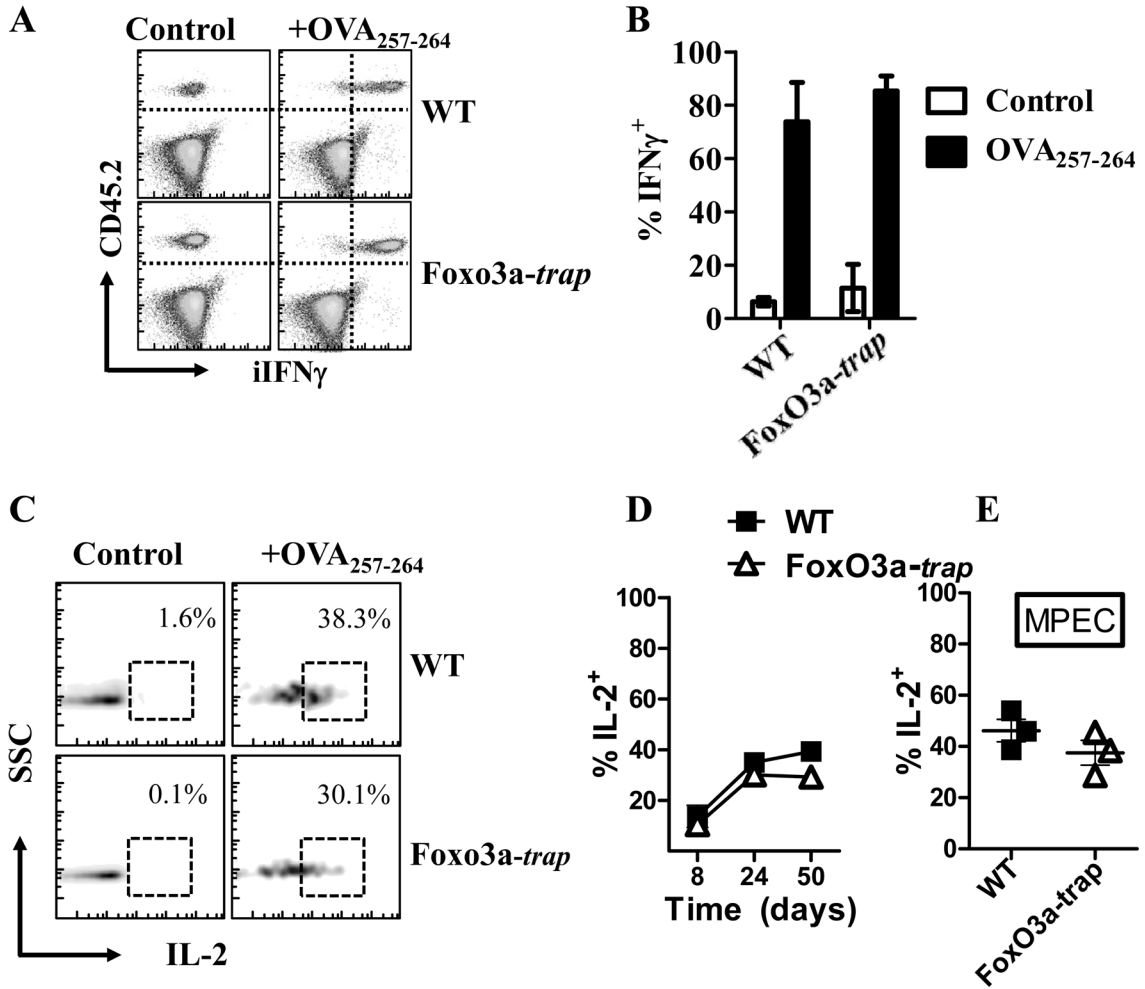**Fig. 5. Reduced apoptosis in FoxO3a-deficient CD8+ T cells**
WT and FoxO3a-deficient mice were infected with 10^4 (i.v) LM-OVA. At day 15 post-infection, cell aliquots were evaluated for Annexin V (A, B) and TUNEL (A, C) staining as described in the methods section. WT and FoxO3a-deficient mice were infected with LM-OVA (10^4, iv) and OVA-specific cells were purified from spleen cells by magnetic selection followed by cell sorting. Purified cells were lysed with RIPA buffer and cell lysates were normalized for cell number (1×10^5 cells). Western blot was performed with anti-Foxo3a, anti-BID, anti-BIM, anti-PUMA and anti-actin antibodies (D–E). Expression of the various molecules was evaluated in relation to actin by densitometry (E). Results are representative of two independent experiments (* *p<0.05*). The expression of Fas (F) was evaluated in OVA-specific CD8+ T cells at day 15 post-infection. Intracelular staining of OVA-specific cells with anti-Bcl2 antibody was performed at day 15 post-infection (G–I).
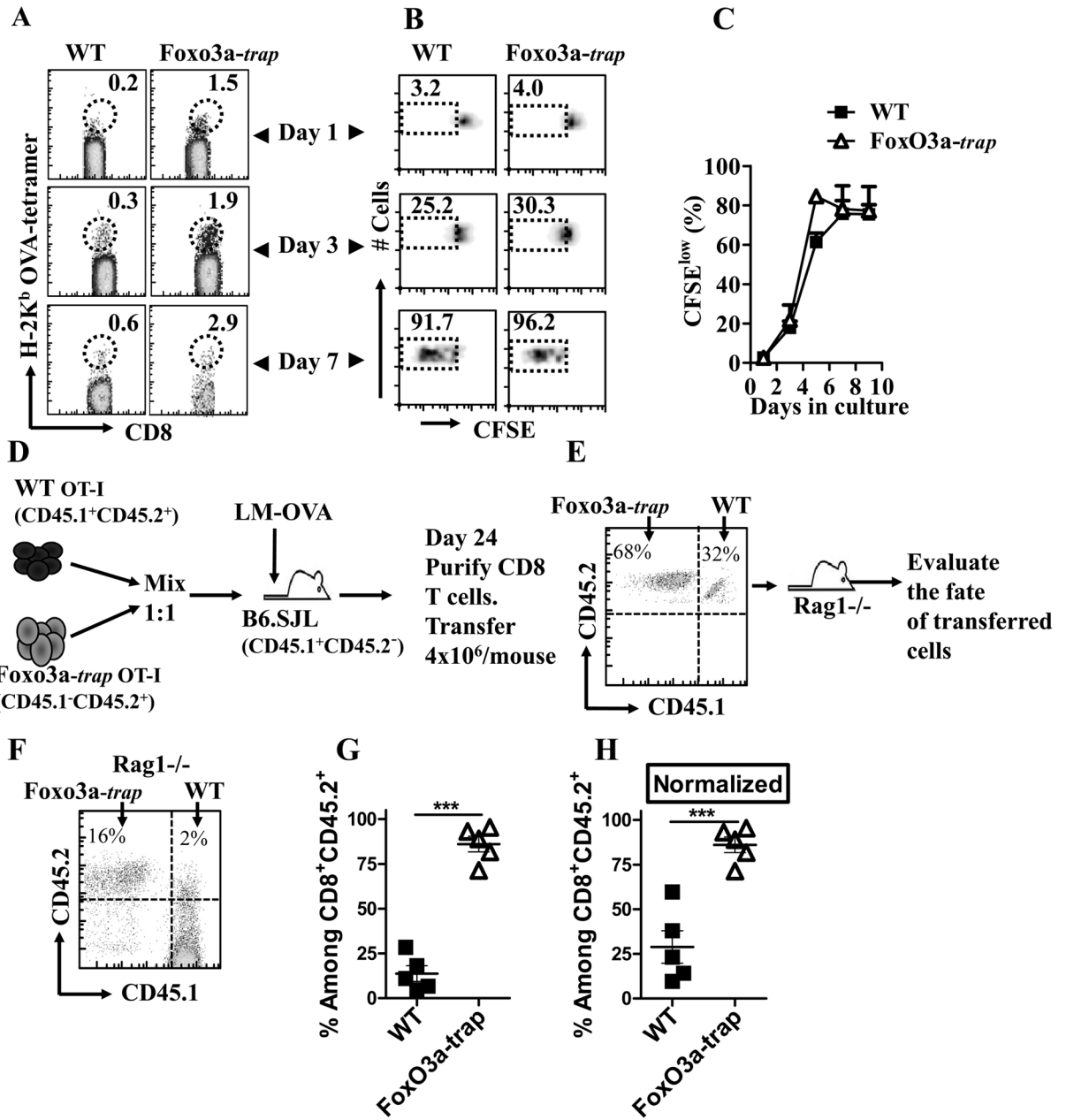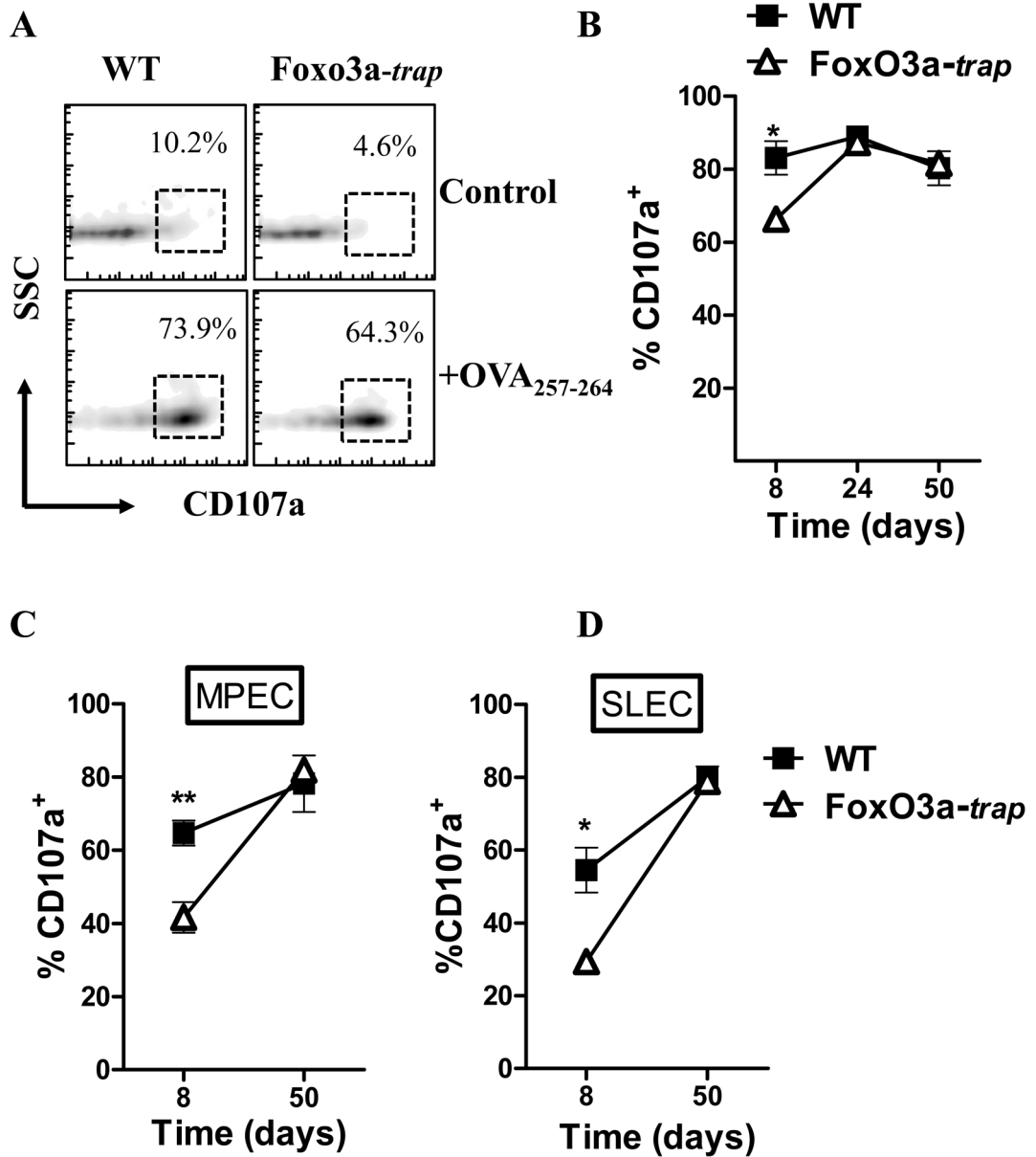
Fig. 6. Enhanced long-term survival of FoxO3a-deficient CD8^{+} T cells in Rag1-deficient hosts
WT and FoxO3a-deficient mice were infected with LM-OVA. At day 30 post-infection, spleens were removed from infected mice and cells stained with CFSE and cultured *in vitro* in the presence of IL-7 (10 ng/ml) and IL-15 (10 ng/ml). At days 1 to 9 of *in vitro* culture, aliquots were stained with anti-CD8 antibody and OVA-tetramer (A, B). Reduction in the expression of CFSE was monitored by Flow cytometry (B, C). WT and FoxO3a-deficient OT-1 cells were mixed 1:1 and injected (iv, 10[4]/mouse) into B6.SJL mice followed by infection with LM-OVA. At day 24, CD8^{+} T cells were purified from recipients and adoptively transferred (iv, 4×10^{6}/mouse) into naïve Rag1-deficient mice (D). The proportion of WT versus FoxO3a-deficient cells that went into Rag1-deficient mice was evaluated (E) and the fate of these cells was then evaluated in mice at thirty days post-transfer (F–H). The

fate of transferred cells was also evaluated when the input numbers of OVA-specific CD8^{+} T cells (WT versus FoxO3a mutant) were normalized (H).

A

Control   +OVA$_{257-264}$

CD45.2

WT

Foxo3a-*trap*

iIFNγ

B

% IFNγ$^+$

□ Control
■ OVA$_{257-264}$

WT   FoxO3a-*trap*

C

Control   +OVA$_{257-264}$

SSC

1.6%   38.3%   WT

0.1%   30.1%   Foxo3a-*trap*

IL-2

D

■ WT
△ FoxO3a-*trap*

% IL-2$^+$

8   24   50
Time (days)

E

% IL-2$^+$

MPEC

WT   FoxO3a-trap

Fig. 7. Expression of intracellular cytokines by WT and FoxO3a-deficient CD8$^+$ T cells
WT and FoxO3a-deficient OT-1 cells were injected (10^4, iv) into naïve B6.SJL mice which
were then challenged with 10^4 LM-OVA (iv) immediately thereafter. At day 60, spleens
were removed from infected mice, stained with anti-CD45.1, anti-CD45.2 and anti-CD8
antibodies. Cells were stimulated *in vitro* with OVA-peptide for 4 h in the presence of Golgi
stop. Cells were permeabilized, stained with antibodies against IFN- (A, B) and IL-2 (C,
D), followed by Flow cytometric evaluation. Cells were also stained with antibodies against
CD127 and KLRG1 to enumerate IL-2 expression by MPECs (E).

A

WT   Foxo3a-*trap*

10.2%   4.6%   Control

SSC

73.9%   64.3%   +OVA$_{257-264}$

CD107a

B

■ WT
△ FoxO3a-*trap*

% CD107a$^+$

Time (days)

C

MPEC

% CD107a$^+$

Time (days)

D

SLEC

%CD107a$^+$

■ WT
△ FoxO3a-*trap*

Time (days)

Fig. 8. Degranulation of CD107a in CD8$^+$ T cells
WT and FoxO3a-deficient OT-1 cells as outlined in Fig. 4C were injected into B6.SJL mice followed by LM-OVA infection. At various time intervals, spleens were removed from infected mice and spleen cells stimulated with OVA-peptide for 4 h in the presence of monensin and anti-CD107a antibody. Cells were then stained with anti-CD45.1, anti-CD45.2 and anti-CD8 antibodies (A, B). Panel A shows the plots at day 8 post-infection. Cells were also stained with antibodies against CD127 and KLRG1 to enumerate CD107a expression in MPECs (C) and SLECs (D).